

# An *ab Initio* Study of the Reactivity of Formylketene. Pseudopericyclic Reactions Revisited

David M. Birney\* and P. Eugene Wagenseller

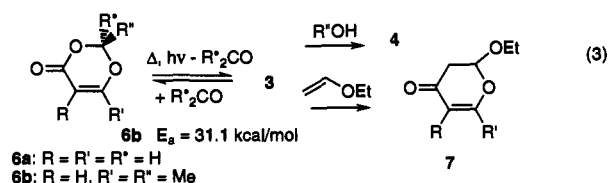
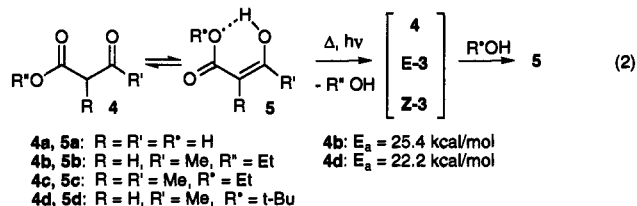
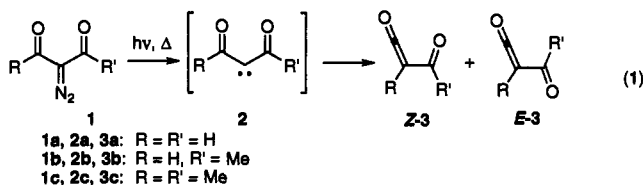
Contribution from the Department of Chemistry and Biochemistry, Texas Tech University, Lubbock, Texas 79409-1061

Received February 22, 1993. Revised Manuscript Received April 28, 1994\*

**Abstract:** Transition structures for the addition of water and formaldehyde to (*Z*)-formylketene ((*Z*)-3a) were studied using *ab initio* calculations. Geometries were optimized at the MP2/6-31G\* level of theory, and energies were calculated at the MP4(SDQ)/6-31G\* level. The barrier for the addition of water to (*Z*)-3a is predicted to be lower (6.3 kcal/mol) than that for the addition of formaldehyde (10.6 kcal/mol), a difference which should provide synthetically useful selectivity. For the ring opening of the  $\beta$ -lactone 15a to (*Z*)-3a, the barrier is lower, only 2.5 kcal/mol. Geometries of the transition structures are early, as expected for exothermic reactions. All of the transition structures are planar, or nearly so, and indicate concerted, slightly asynchronous reactions. The orbital symmetry rules are irrelevant to these planar structures. Analysis of the molecular orbitals indicates that the reactions are orbital symmetry allowed and are best described as pseudopericyclic. This concept is discussed in detail and provides an explanation of the remarkably low barriers for these reactions as compared to model pericyclic reactions.

## Introduction

The simplest  $\alpha$ -oxo ketene, formylketene (3a), is generated by the Wolff rearrangement of the diketocarbene 2a, in turn obtained from diazomalonaldehyde (1a) (eq 1).<sup>1</sup> A number of substituted  $\alpha$ -oxo ketenes have been observed in matrices and/or proposed as intermediates.<sup>2</sup> In addition to the Wolff rearrangement, other common modes of preparation include the thermal or photochemical elimination of HOR from  $\beta$ -ketoesters (4) via the enol (5)<sup>2a,b,n</sup> (eq 2) and the extrusion of acetone from 2,2-dimethyl-4*H*-1,3-dioxin-4-ones (e.g., 6b),<sup>2a,h,i,3</sup> (eq 3). A stable, hindered  $\alpha$ -oxo ketene has been shown by X-ray crystallography to adopt the *E*-conformation.<sup>21</sup> It has been suggested that its stability arises because it is prevented from adopting the *Z*-conformation, which is required for the concerted [4 + 2] cycloaddition.<sup>2h,4</sup> Witzeman has measured the activation parameters for the formation of acetylketene (3a) by the pyrolysis of substituted  $\beta$ -ketoesters (4b and c, eq 2)<sup>28</sup> and 2,2,6-trimethyldioxin-4-one (6b, eq 3)<sup>26</sup> with 1-butanol in xylene. These are both unimolecular reactions in which the rate-determining step is the formation of a reactive intermediate, presumably acetylketene. The rates are independent of the nature or concentration of added nucleophilic trapping reagents, which included alcohols, ketones, and enol ethers, giving 4, 6, and 7, respectively (eq 3). The reactions are carried out in nonpolar solvents, typically xylene, with no added



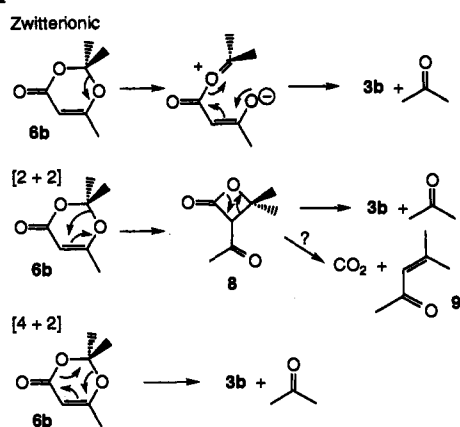
\* Abstract published in *Advance ACS Abstracts*, June 1, 1994.  
(1) (a) Arnold, Z.; Sauliova, J. *Collect. Czech. Chem. Commun.* **1973**, *38*, 2641-2647. (b) Maier, G.; Reisenauer, H. P.; Sayrac, T. *Chem. Ber.* **1982**, *115*, 2192-2201. (c) Wenkert, E.; Ananthanarayan, T. P.; Ferreira, V. F.; Hoffmann, M. G.; Kim, H. *J. Org. Chem.* **1990**, *55*, 4975-4976.  
(2) (a) Newman, M. S.; Zuech, E. A. *J. Org. Chem.* **1962**, *27*, 1436. (b) Jager, G. *Chem. Ber.* **1965**, *98*, 1184. (c) Ulrich, H. *Cycloaddition Reactions of Heterocumulenes*; Academic Press: New York, 1967; Vol. 9, pp 38-109. (d) Hyatt, J. A.; Feldman, P.; Clemens, R. J. *J. Org. Chem.* **1984**, *49*, 5105-5108. (e) Clemens, R. J.; Witzeman, J. S. *J. Am. Chem. Soc.* **1989**, *111*, 2186-2193. (f) Allen, A. D.; Gong, L.; Tidwell, T. T. *J. Am. Chem. Soc.* **1990**, *112*, 6396-6397. (g) Witzeman, J. S. *Tetrahedron Lett.* **1990**, *31*, 1401-1404. (h) Freiermuth, B.; Wenstrup, C. *J. Org. Chem.* **1991**, *56*, 2286-2289. (i) Emerson, D. W.; Titus, R. L.; Gonzales, R. M. *J. Org. Chem.* **1991**, *56*, 5301. (j) Witzeman, J. S.; Nottingham, W. D. *J. Org. Chem.* **1991**, *56*, 1713-1718. (k) Gong, L.; McAllister, M. A.; Tidwell, T. T. *J. Am. Chem. Soc.* **1991**, *113*, 6021-6028. (l) Kappe, C. O.; Evans, R. A.; Kennard, C. H. L.; Wenstrup, C. *J. Am. Chem. Soc.* **1991**, *113*, 4234-4237. (m) Leung-Toung, R.; Wenstrup, C. *J. Org. Chem.* **1992**, *57*, 4850-4858. (n) Coleman, R. S.; Fraser, J. R. *J. Org. Chem.* **1993**, *58*, 385-392.  
(3) Kaneko, C.; Sato, M.; Sakaki, J.-i.; Abe, Y. *J. Heterocycl. Chem.* **1990**, *27*, 25.  
(4) Allen, A. D.; McAllister, M. A.; Tidwell, T. T. *Tetrahedron Lett.* **1993**, *34*, 1095-1098.

catalyst and show no appreciable solvent effect. The observation that fragmentation of the more sterically hindered *tert*-butyl ester 4d proceeds faster than that of the ethyl ester 4b (eq 2) is consistent with rate-determining elimination to form the  $\alpha$ -oxo ketene 3b, followed by rapid addition to give the products.

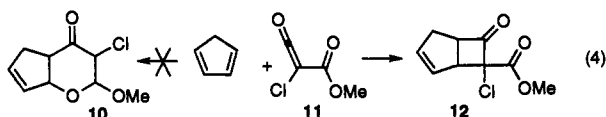
What are the mechanisms of formation of acetylketene from dioxinone 6b and  $\beta$ -ketoester 4d? Three possibilities (stepwise zwitterionic, [2 + 2] cycloreversion, and [4 + 2] cycloreversion) for the former reaction are outlined in Scheme 1. The reaction of imines with ketenes has been shown to proceed via a zwitterion.<sup>5,6</sup> However, the stepwise zwitterionic pathway is

(5) (a) Moore, H. W.; Hernandez, L., Jr.; Chambers, R. *J. Am. Chem. Soc.* **1978**, *100*, 2245-2247. (b) Palomo, C.; Cossio, F. P.; Odiozola, J. M.; Oiarbide, M.; Ontoria, J. M. *J. Org. Chem.* **1991**, *56*, 4418-4428. (c) Sordo, J. A.; Gonzalez, J.; Sordo, T. L. *J. Am. Chem. Soc.* **1992**, *114*, 6249-6251. (d) Cossio, F. P.; Ugaldé, J. M.; Lopez, X.; Lecea, B.; Palomo, C. *J. Am. Chem. Soc.* **1993**, *115*, 995-1004.

## Scheme 1



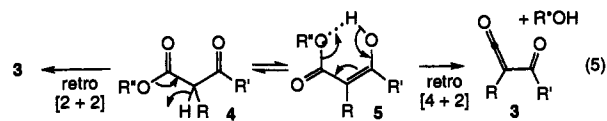
unlikely for reactions of either **4d** or **6b**, in view of the lack of a requirement for added catalysts (acid or base) or a solvent effect. Indeed, the unimolecular fragmentation reactions of **4d** and **6b** occur with equal ease in solution and in the gas phase.<sup>2c,g,h,j,m</sup> Additions to (alkoxycarbonyl)ketenes (e.g., **11**) yield products from [2 + 2] cycloadditions (e.g., **12**, eq 4).<sup>9</sup> This may be because



the product from the [4 + 2] cycloaddition (e.g., **10**) would have lost the internal resonance of the ester.<sup>10,11</sup> In contrast, the experimental evidence summarized below suggests that additions to other  $\alpha$ -oxo ketenes give products from [4 + 2] cycloadditions.

For the formation of **3b** from **6b**, the [4 + 2] cycloreversion (Scheme 1) is the simplest alternative, giving **3b** directly in one step. The [2 + 2] cycloreversion seems unlikely in this case, because it would require a preliminary [1,3] sigmatropic rearrangement, which is forbidden, to give **8** as an intermediate. While this mechanism is, in principle, consistent with the observed kinetics and lack of solvent effect, only acetylketene and acetone are observed in the argon matrix, and not **8**. Furthermore, if **8** is an intermediate, it would be expected to fragment to the more stable products,  $\text{CO}_2$  and **9**,<sup>12</sup> rather than lose acetone as observed to give **3b**.

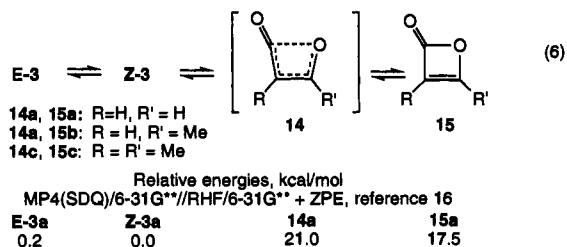
Interpretation of the chemistry of  $\beta$ -ketoesters **4** is complicated by the enol tautomer **5**. The [2 + 2] cycloreversion mechanism in eq 5 provides the most direct route to  $\alpha$ -oxo ketenes (**3**). However, when the equilibrium mixture of the keto and enol forms of the  $\beta$ -ketoester **4d** was pyrolyzed in the gas phase (where tautomerization is slow) and trapped in an argon matrix, a mixture of unreacted  $\beta$ -ketoester **4d**, *tert*-butyl alcohol, and both the *E*



and *Z* forms of acetylketene (**3b**) but none of the enols **5a** or **5b** was observed (eq 2).<sup>2a,h,13</sup> Furthermore, when a matrix containing both acetylketene (**3b**) and an alcohol is warmed to between  $-90$  and  $-50$  °C, the acetylketene undergoes a facile reaction with the alcohol to form only the enol (**5b**) and none of the keto tautomer (**4b**). Thus, a concerted pericyclic<sup>14</sup> [4 + 2] fragmentation of the enol tautomer **5** (eq 5) is consistent with all the experimental evidence.

In summary, a concerted mechanism is consistent with the experimental observations that these fragmentations to form  $\alpha$ -oxo ketenes (eqs 2 and 3) are unimolecular, do not require catalysts, show no solvent effects, and readily occur in the gas phase. The intermediacy of a zwitterion is inconsistent with these observations. Furthermore, in those cases for which there might be some ambiguity, the evidence favors the [4 + 2] pathway over the [2 + 2] process. It was this unusual reactivity of  $\alpha$ -oxo ketenes, in contrast to the more common [2 + 2] reactions of ketenes,<sup>2c</sup> which prompted this *ab initio* study on the concerted [4 + 2] reactions of formylketene (**3a**) with the aim of elucidating those electronic factors which permit this mode of reactivity.

**Previous Calculations.** There have been several calculations reported on  $\alpha$ -oxo ketenes, but none deal with the mechanism of their addition reactions. Those of Nguyen, Ha, and More O'Ferrall on formylketene (**3a**), summarized in eq 6, are of particular relevance.<sup>16</sup> Their results (MP4(SDQ)/6-31G\*\* ener-



gies at RHF/6-31G\*\* geometries with zero-point vibrational energy corrections) indicate that (*Z*)-**3a** is slightly stabilized (0.2 kcal/mol) relative to (*E*)-**3a**, but they do not discuss the origin of this preference. The  $\beta$ -lactone **15c** has been proposed as an intermediate in the reaction of atomic carbon with 2,3-butane-dione. (The observed products are  $\text{CO}_2$  and 2-butyne).<sup>12a</sup> Nguyen et al. located a transition structure (**14a**) for this proposed ring opening which is completely planar and is only 3.5 kcal/mol above **15a**. Although the authors do not comment on it, the planarity of this transition structure is in remarkable contrast to all other transition structures reported for electrocyclic ring openings of cyclobutenes, which generally require a twisting of the ends of the breaking  $\sigma$ -bond so that the orbitals can overlap with the

(6) The formation of  $\beta$ -lactams from the reaction of imines and diketene has been proposed to be a concerted [2 + 2] cycloaddition between **3b** and the imine.<sup>7</sup> However, other workers have shown that similar reactions involve a zwitterionic intermediate.<sup>5,8</sup>

(7) Kawabata, T.; Kimura, Y.; Ito, Y.; Terashima, S.; Sasaki, A.; Sunagawa, M. *Tetrahedron* **1988**, *44*, 2149–2165.

(8) Ghosez, L.; O'Donnell, M. J. In *Pericyclic Reactions*; Marchand, A. P., Lehr, R. E., Eds.; Academic Press: New York, 1977; Vol. 2, pp 79–141.

(9) (a) Goldstein, S.; Vannes, P.; Houge, C.; Frisque-Hesbain, A. M.; Wiaux-Zamar, C.; Ghosez, L.; Germain, G.; Declercq, J. P.; Meerssche, M. V.; Arrieta, J. M. *J. Am. Chem. Soc.* **1981**, *103*, 4616–4618. (b) Stevens, R. V.; Bisacchi, G. S.; Goldsmith, L.; Strouse, C. E. *J. Org. Chem.* **1980**, *45*, 2708–2709.

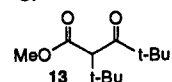
(10) Wiberg, K. B.; Laidig, K. E. *J. Am. Chem. Soc.* **1987**, *109*, 5935–5943.

(11) Conjugation of a ketene with an acid group is calculated to be 1.1 kcal/mol more stabilizing than conjugation of a ketene with a formyl group.<sup>2f</sup>

(12) (a) Biesiada, K. A.; Shevlin, P. B. *J. Org. Chem.* **1984**, *49*, 1151–1153.

(b) Hagemeyer, H. J. *Ind. Eng. Chem.* **1949**, *41*, 765. (c) Kresze, G.; Trede, A. *Tetrahedron* **1963**, *19*, 133. (d) Staudinger, H. *Die Ketene*; Enke: Stuttgart, 1912. (e) Chapman, O. L.; McIntosh, C. L.; Pacansky, J. *J. Am. Chem. Soc.* **1973**, *95*, 245.

(13) Wentrup et al. report that "those esters which do not readily enolize react very sluggishly (to give  $\alpha$ -oxo ketenes); the reaction product containing the ketene is rich in the keto form and depleted of enol (of the reactant)." This was particularly true for compound **13**, which exists primarily in the keto form at room temperature and for which no ketene was detected until the pyrolysis temperature was above 400 °C.<sup>2b</sup>



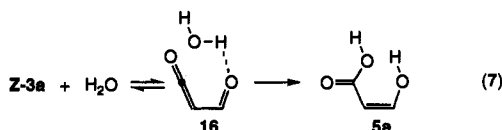
(14) According to the Woodward–Hoffmann definition, "reactions in which all first-order changes in bonding relationships take place in concert on a closed curve".<sup>15</sup>

(15) Woodward, R. B.; Hoffmann, R. *The Conservation of Orbital Symmetry*; Verlag Chemie, GmbH: Weinheim, 1970.

(16) Nguyen, M. T.; Ha, T.; More O'Ferrall, R. A. *J. Org. Chem.* **1990**, *55*, 3251–3256.

$\pi$ -system.<sup>15,17</sup> The significance of this planarity will be discussed below in the context of pseudopericyclic reactions.

Tidwell et al. have performed RHF/6-31G\* calculations on formylketene.<sup>2f,k</sup> Isodesmic reactions indicate that the formyl substituent stabilizes ketene by 3.6 kcal/mol through the  $\pi$ -acceptor ability of the aldehyde. After this paper was submitted, Tidwell reported RHF/6-31G\* calculations on the structures of formylketene (3a), a complex between 3a and water (16), and the addition product 3-hydroxypropenoic acid (5a, eq 7).<sup>4</sup> They found that at the RHF/3-21G level, there was no barrier to the addition of water to 3a, but at the RHF/6-31G\* level, complex 16 could be located.



There have been many theoretical studies reported on [2 + 2] reactions of ketene.<sup>5c,18</sup> Those at the highest level are by Bernardi et al.<sup>18a</sup> and Wang and Houk,<sup>18b</sup> who have investigated the addition of ketene to ethene at the MCSCF and MP2/6-31G\* levels, respectively. Both groups have located concerted but very asynchronous transition structures in which there is strong bonding between the central carbon of the ketene and both carbons of the ethene. The second bond is formed past the transition state. The MP2/6-31G\* activation energy of 26.7 kcal/mol is somewhat below the experimental value of 32.0 kcal/mol.<sup>19</sup> There are no previous calculations on [4 + 2] cycloadditions of ketenes in which ketene acts as a dienophile or in which a substituted ketene acts as a diene. A very shallow minimum corresponding to an extended zwitterionic intermediate was located at both the RHF/6-31G\* and MP2/6-31G\* levels in the reaction of ketene with imine in work by Sordo et al.<sup>5c</sup>

### Computational Details

The *ab initio* calculations were carried out with the GAUSSIAN 88 and 90 suites of programs, using standard basis sets.<sup>20</sup> Structures were optimized in *C<sub>s</sub>* symmetry at both the RHF/3-21G and RHF/6-31G\* levels using standard gradient techniques. The structures obtained were confirmed as minima by frequency calculations. In all subsequent discussions of calculated zero-point vibrational energies (ZPE), the RHF/6-31G\* values have been scaled by a factor of 0.9 to compensate for the well-documented tendency of the RHF/6-31G\* level to overestimate the steepness of potential energy wells and hence the vibrational frequencies. The empirical scaling factor of 0.9 is commonly used to bring the calculated vibrational frequencies into closer agreement with experimental values.<sup>21</sup> Unless otherwise noted, all structures were further optimized at the MP2/6-31G\*(full) level, a method which recovers some of the effects of electron correlation on the structures. This can be of particular importance for the energies of transition structures and has been shown to reproduce the

activation energies for a range of concerted pericyclic reactions.<sup>18b,22</sup> Unless otherwise noted, all energies discussed below are MP4(SDQ)/6-31G\* single-point energies (frozen core, MP4 with single, double, and quadruple excitations) at the MP2/6-31G\* optimized geometries and with scaled ZPE corrections from frequency calculations of the RHF/6-31G\* optimized structures. Optimized Cartesian coordinates for all structures are available in the supplemental material.

### Results and Discussion

Geometry optimized structures were obtained for all the reactants, transition structures, and products and are shown in Figure 1. The atom numbering in all the structures is based on that for formylketene (3a), for atoms 1–7. In the addition reactions, the two atoms directly involved in bonding to the 3a substructure are consistently numbered 8 and 9. The calculated energies of these structures are recorded in Table 1, and their relative energies in specific reactions are presented in Table 2. Inspection of Table 2 shows that the usual trends are observed in calculated activation energies,<sup>22</sup> specifically that the RHF method overestimates the activation energy, MP2 underestimates it, and then MP3 and MP4 begin to converge on a reasonable activation energy.

**Addition of Water to Formylketene.** Although kinetic data are available only for more highly substituted systems, the reactions of formylketene (3a) were studied because the number of atoms involved makes calculations of larger systems impractical. For the fragmentation of the enols of the acetoacetate esters 5b and 5d to form acetylketene (3b) and an alcohol (eq 2), the [4 + 2] cycloreversion of 5a to form water and 3a (eq 7) is a reasonable model which preserves the essential electronic aspects of the reaction. The experimental activation energy for the fragmentation of *tert*-butyl acetoacetate (4d, 22.19 kcal/mol) is slightly lower than that for the ethyl ester (4b, 25.43 kcal/mol).<sup>28</sup> Witzeman suggested that this is due to relief of steric crowding in the ground state of the *tert*-butyl ester. Thus, by the Bell-Evans-Polanyi principle<sup>23</sup> and the Hammond Postulate,<sup>24</sup> the calculated activation energy for the reaction of the less sterically crowded acid 5a would be expected to be somewhat higher than the experimentally measured value for either of the esters 4a or 4b.

The ground-state geometry of 5a (Figure 1A) was optimized in *C<sub>s</sub>* symmetry at the RHF/3-21G, RHF/6-31G\*, and MP2/6-31G\* levels. A grid search for the transition structure, with fixed C<sub>2</sub>-O<sub>8</sub> bond distances, confirmed the results of Tidwell et al.;<sup>4</sup> at the RHF/3-21G level, there is no calculated barrier for the addition of water to formylketene. This result is surprising because there are experimental barriers to the addition of water to ketenes<sup>25</sup> and because most pericyclic reactions have substantial barriers.<sup>22a</sup> Furthermore, in most calculations of transition structures for pericyclic reactions, the RHF/3-21G level *overestimates* the height of the barrier.<sup>17b,21a,22</sup>

Polarization functions are particularly important for accurately representing bonds involving electronegative atoms.<sup>21a</sup> A transition structure 17 was successfully located at the RHF/6-31G\* level. Since it is unusual for the 3-21G and 6-31G\* basis sets to give such qualitatively different potential energy surfaces at the RHF level,<sup>21a,22</sup> we optimized the structures (5a and 17 in Figure 1A and 3a in Figure 1C) at the MP2/6-31G\* level, thus probing the importance of electron correlation. These geometries are essentially the same as the RHF/6-31G\* ones. The MP2/6-31G\* energy of the transition structure 17 was 5.6 kcal/mol

(22) (a) Houk, K. N.; Li, Y.; Evanseck, J. D. *Angew. Chem., Int. Ed. Engl.* **1992**, *31*, 682–708. (b) Birney, D. M.; Wiberg, K. B.; Berson, J. A. *J. Am. Chem. Soc.* **1988**, *110*, 6631–6642. (c) Jensen, F.; Houk, K. N. *J. Am. Chem. Soc.* **1987**, *109*, 3139–3140.

(23) (a) Bell, R. P. *Proc. R. Soc. London, Ser. A* **1936**, *154*, 414. (b) Evans, M. G.; Polanyi, M. *Trans. Faraday Soc.* **1938**, *34*, 11–29.

(24) Hammond, G. S. *J. Am. Chem. Soc.* **1955**, *77*, 334.

(25) Blake, P. In *The Chemistry of Ketenes, Allenes, and Related Compounds, Part 1*; Patai, S., Ed.; John Wiley and Sons: New York, 1980; pp 309–362.

(17) (a) Kallel, E. A.; Wang, Y.; Houk, K. N. *J. Org. Chem.* **1989**, *54*, 6006. (b) Spellmeyer, D. C.; Houk, K. N. *J. Am. Chem. Soc.* **1988**, *110*, 3412. (c) Rudolf, K.; Spellmeyer, D. C.; Houk, K. N. *J. Org. Chem.* **1987**, *52*, 3708–3710.

(18) (a) Bernardi, F.; Bottoni, A.; Robb, M. A.; Venturini, A. *J. Am. Chem. Soc.* **1990**, *112*, 2106–2114. (b) Wang, Z.; Houk, K. N. *J. Am. Chem. Soc.* **1990**, *112*, 1754–1756. (c) Schaad, L. J.; Gutman, I.; Hess, B. A., Jr.; Hu, J. *J. Am. Chem. Soc.* **1991**, *113*, 5200–5203. (d) Seidl, E. T.; Schaefer, H. F., III. *J. Am. Chem. Soc.* **1991**, *113*, 5195–5200.

(19) (a) Das, M. N.; Kern, F.; Coyle, T. D.; Walters, W. D. *J. Am. Chem. Soc.* **1954**, *76*, 6271. (b) McGee, T. H.; Schliefer, A. *J. Phys. Chem.* **1972**, *76*, 963.

(20) Frisch, M. J.; Head-Gordon, M.; Trucks, G. W.; Foresman, J. B.; Schlegel, H. B.; Raghavachari, K.; Robb, M.; Binkley, J. S.; Gonzalez, C.; Defrees, D. J.; Fox, D. J.; Whiteside, R. A.; Seeger, R.; Melius, C. F.; Baker, J.; Martin, R. L.; Kahn, L. R.; Stewart, J. J. P.; Topiol, S.; Pople, J. A. *Gaussian 90*; Gaussian, Inc.: Pittsburgh, PA, 1990.

(21) (a) Hehre, W. J.; Radom, L.; Schleyer, P. v. R.; Pople, J. A. *Ab Initio Molecular Orbital Theory*; John Wiley and Sons: New York, 1986. (b) Hess, A. B., Jr.; Schaad, L. J.; Polavara, P. L. *J. Am. Chem. Soc.* **1984**, *106*, 4348.

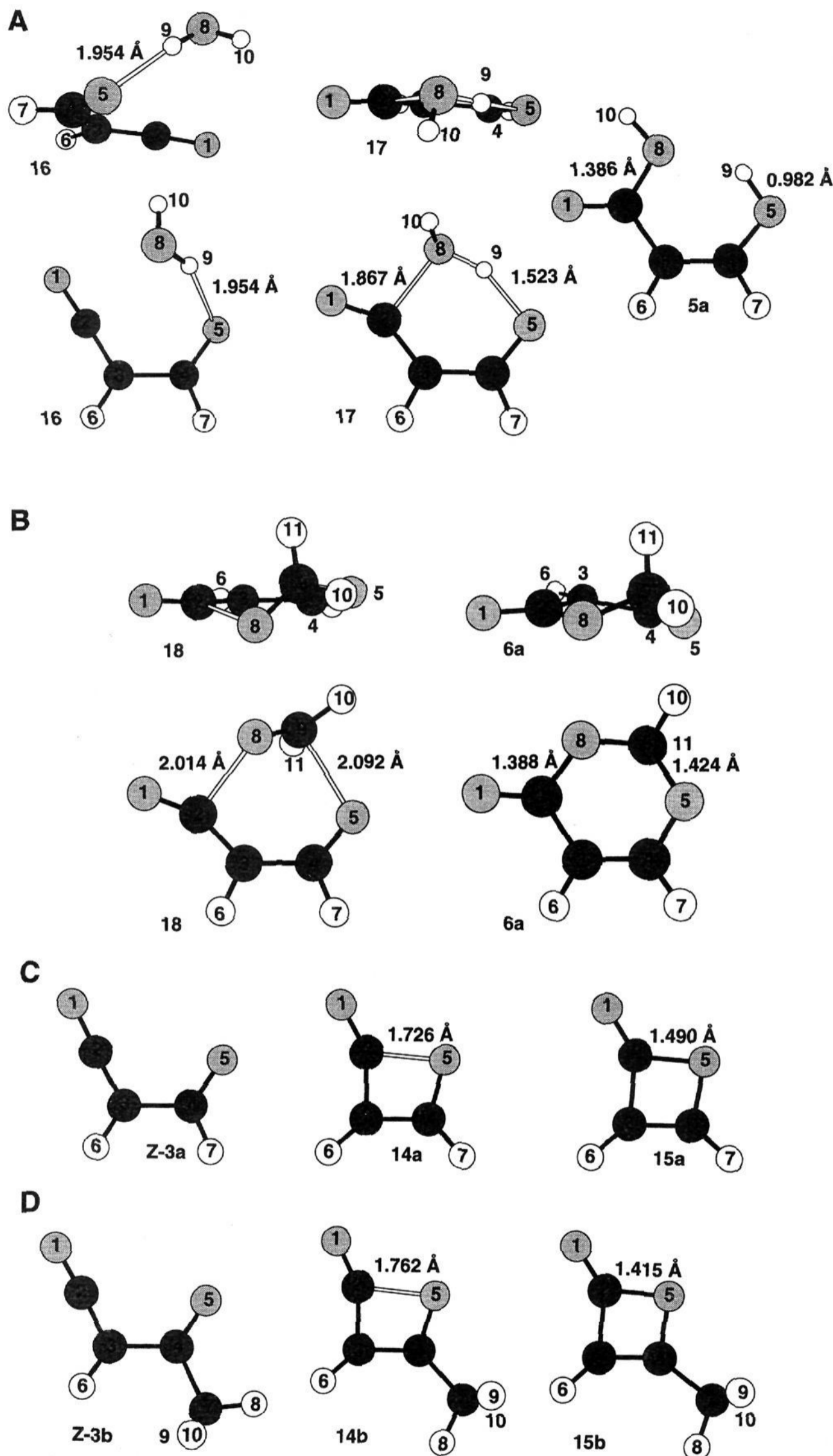


**Figure 1.** Views of the optimized structures (*Z*)-3a, (*Z*)-3b, 5a, 6a, 14a, 14b, 15a, 15b, 16, 17, and 18. Structures with  $C_s$  symmetry are shown in top view only. Structures with  $C_1$  symmetry are shown in top and side views. All structures were optimized at the MP2/6-31G\* level, with the exception of (*Z*)-3b, 14b, and 15b, which were optimized at the RHF/6-31G\* level. Partial bonds are unfilled. Hydrogens are unshaded, oxygens have light shading, and carbons have dark shading. Atom numbering is based on 3a. (A) Addition of water to 3a. (B) Addition of formaldehyde to 3a. (C) Ring closure of 3a to 15a. (D) Ring closure of 3b to 15b.

below that of the reagents 3a plus water (2.8 kcal/mol with the ZPE correction).<sup>26</sup> This is reminiscent of the gas-phase potential energy surface for the  $S_N2$  reaction,<sup>27</sup> and the requisite inter-

molecular complex was located at both the RHF/6-31G\* and MP2/6-31G\* levels (16, Figure 1A), 13.6 and 2.1 kcal/mol, respectively, below the reactants with the ZPE correction. The

**Table 1.** Absolute Energies (hartrees), Zero-Point Vibrational Energy Contributions (ZPE; kcal/mol), and the Lowest Frequency ( $\text{cm}^{-1}$ ) or Imaginary Frequency of Reactants, Products, and Transition Structures, Optimized at the RHF/6-31G\* Level (Absolute MP2/6-31G\*, MP3/6-31G\* and MP4(SDQ)/6-31G\* Energies, at the RHF/6-31G\* and MP2/6-31G\* Optimized Geometries)

structure	RHF/6-31G* geometry			MP2/6-31G* geometry			
	RHF/6-31G* energy	ZPE <sup>a</sup>	low frequency <sup>b</sup>	MP2/6-31G* <sup>c</sup> energy	MP2/6-31G* energy	MP3/6-31G* <sup>c</sup> energy	MP4(SDQ)/6-31G* <sup>c</sup> energy
Addition of Water to 3a, Figure 1A, 2							
(Z)-3a	-264.457 35	29.3	164	-265.172 08	-265.198 17	-265.175 18	-265.195 56
H <sub>2</sub> O	-76.010 75	14.4	1827	-76.195 93	-76.199 24	-76.202 05	-76.204 97
16	-340.476 62	45.5	58	-341.379 42	-341.409 37	-341.388 52	-341.411 74
17	-340.456 94	46.9	390i	-341.376 63	-341.406 38	-341.380 14	-341.403 57
5a	-340.518 67	50.1	104	-341.419 51	-341.448 03	-341.433 85	-341.451 69
5a'	-340.525 16	50.2	127	-341.425 97	-341.454 40	-341.440 00	-341.457 57
Addition of Formaldehyde to 3a, Figure 1B							
CH <sub>2</sub> O	-113.866 33	18.3	1336	-114.165 26	-114.174 96	-114.172 89	-114.181 63
18	-378.299 13	50.8	487i	-379.332 27	-379.366 78	-379.333 69	-379.364 80
6a	-378.372 71	55.1	155	-379.391 13	-379.425 51	-379.407 91	-379.428 23
Ring Opening of 15a To Yield 3a, Figure 1C							
15a	-264.423 22	30.2	301	-265.159 10 <sup>d</sup>	-265.168 65	-265.150 39	-265.166 78
14a	-264.411 48	28.9	631i	-265.157 02 <sup>d</sup>	-265.166 75	-265.140 92	-265.160 94
(E)-3a	-264.455 88	29.2	166	-265.171 33	-265.197 31	-265.174 81	-265.194 86
Ring Opening of 15b To Yield 3b, Figure 1D							
15b	-303.474 67	48.8	157	-304.325 20		-304.339 10 <sup>e</sup>	-304.355 37 <sup>e</sup>
14b	-303.462 89	47.4	600i	-304.322 21		-304.327 99 <sup>e</sup>	-304.348 23 <sup>e</sup>
(Z)-3b	-303.503 96	47.9	97	-304.349 34		-304.359 94 <sup>e</sup>	-304.379 46 <sup>e</sup>

<sup>a</sup> Calculated from the RHF/6-31G\* frequencies (unscaled). <sup>b</sup> In  $\text{cm}^{-1}$ . The transition structures had one and only one imaginary frequency, the displacements of which corresponded to the reaction coordinate. <sup>c</sup> Calculated using the frozen core approximation. <sup>d</sup> MP2/6-31G\*\*//RHF/6-31G\* from ref 16. <sup>e</sup> Calculated at the RHF/6-31G\* geometry.

**Table 2.** Relative Energies (kcal/mol) of Transition Structures, Reactant, and Products Optimized at the RHF/6-31G\* and MP2/6-31G\* Levels (Additional Energy Differences ( $\Delta E$ ) Are Given between Selected Structures)

structure	RHF/6-31G* geometry		MP2/6-31G* geometry			
	RHF/6-31G*	MP2/6-31G* <sup>a</sup>	MP2/6-31G*	MP3/6-31G*	MP4(SDQ) <sup>a</sup> 6-31G*	MP4(SDQ) <sup>a</sup> + ZPE <sup>b</sup>
Addition of Water to 3a, Figures 1A, 2						
(Z)-3a + H <sub>2</sub> O	35.8	36.4	35.8	39.4	35.8	29.9
16	30.5	29.2	28.3	32.3	28.8	24.5
17	42.8	31.0	30.1	37.6	33.9	30.9
$\Delta E$ , (Z)-3a + H <sub>2</sub> O to 17	7.0	-5.4	-5.6	-1.8	-1.9	0.9
$\Delta E$ , 16 to 17	12.4	1.8	1.9	5.3	5.1	6.3
5a	4.1	4.0	4.0	3.9	3.7	3.6
5a'	0.0	0.0	0.0	0.0	0.0	0.0
Addition of Formaldehyde to 3a, Figure 1B						
(Z)-3a + CH <sub>2</sub> O	30.8	33.8	32.9	37.6	32.0	25.3
18	46.7	36.9	36.9	46.6	39.8	35.9
6a	0.0	0.0	0.0	0.0	0.0	0.0
$\Delta E$ , (Z)-3a + CH <sub>2</sub> O to 18	15.9	3.1	4.0	9.0	7.8	10.6
Ring Opening of 15a To Yield 3a, Figure 1C						
15a	21.4	18.0 <sup>c</sup>	18.5	15.6	18.1	18.9
14a	28.8	19.3 <sup>c</sup>	19.7	21.5	21.7	21.4
(Z)-3a	0.0	0.0 <sup>c</sup>	0.0	0.0	0.0	0.0
(E)-3a	0.9	0.5 <sup>c</sup>	0.5	0.2	0.4	0.4
$\Delta E$ , 15a to 14a	7.4	1.3 <sup>c</sup>	1.2	5.9	3.7	2.5
Ring Opening of 15b To Yield 3b, Figure 1D						
15b	18.4	15.1		13.1 <sup>d</sup>	15.1 <sup>d</sup>	15.9 <sup>d</sup>
14b	25.8	17.0		20.0 <sup>d</sup>	19.6 <sup>d</sup>	19.1 <sup>d</sup>
(Z)-3b	0.0	0.0		0.0 <sup>d</sup>	0.0 <sup>d</sup>	0.0 <sup>d</sup>
$\Delta E$ , 15b to 14b	7.4	1.9		7.0 <sup>d</sup>	4.5 <sup>d</sup>	3.2 <sup>d</sup>

<sup>a</sup> Calculated using the frozen core approximation. <sup>b</sup> Zero-point vibrational energy correction from RHF/6-31G\* frequencies and scaled by 0.9. <sup>c</sup> MP2/6-31G\*\*//RHF/6-31G\* from ref 16. <sup>d</sup> Calculated at the RHF/6-31G\* geometry.

geometry of the complex 16 shows no significant distortions from that of the uncomplexed ketene 3a (Figures 2A and 2C). The water is located above the plane of the formylketene but in close proximity to the ketene carbon to which it will add. Single-point energy calculations at the MP4(SDQ)/6-31G\*\*//MP2/6-31G\*

(26) The ZPE correction raises the barrier because two of the three translational degrees of freedom between the reactants are converted into real frequencies at the transition structure. The third degree of freedom becomes the transition vector, which does not contribute to the zero-point vibrational energy.

(27) Chandrasekhar, J.; Smith, S. F.; Jorgensen, W. L. *J. Am. Chem. Soc.* 1985, 107, 154-163.

+ ZPE level place the reactant 0.9 kcal/mol below the transition structure 17 and predict that the complex 16 is 5.4 kcal/mol more stable than the reactants, with an activation energy of 6.3 kcal/mol for the formation of 5a from 16.<sup>28</sup> The complete potential energy surface for this reaction surface is summarized in Figure 2.

One additional point on the potential energy hypersurface has been examined. The rotamer of the hydroxy acid 5a' was anticipated to be more stable than the reactive conformation 5a

(28) There are likely to be other such hydrogen-bonded complexes which were not located, some of which might be lower in energy than 16.

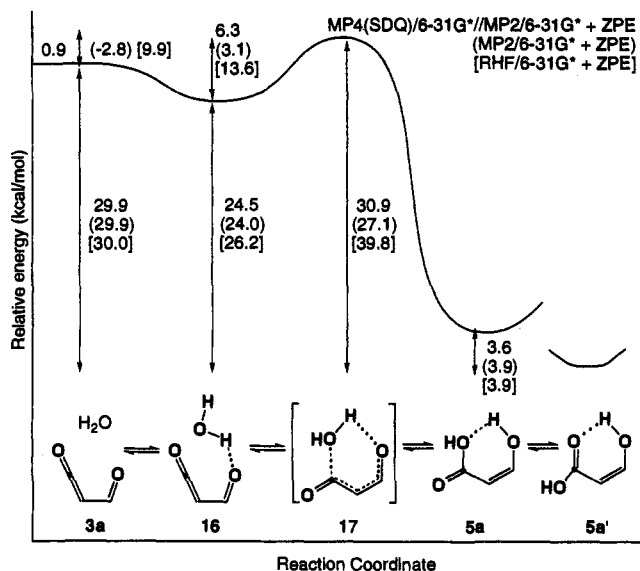


**Figure 2.** Potential energy surface for the reaction of water and formylketene with energies calculated at the MP4(SDQ)//6-31G\*\*/MP2/6-31G\* + ZPE level, showing all the stationary points located in this work. The relative energies at the MP2/6-31G\* + ZPE and RHF/6-31G\* + ZPE levels are also shown. Numbers may not add due to rounding. Note that at the MP2/6-31G\* level, 17 is calculated to be lower in energy than the isolated reactants.

due to stronger hydrogen bonding. This was indeed the case; rotamer 5a' is 3.6 kcal/mol more stable than 5a (see Figure 2).<sup>29</sup>

The low activation energy (6.3 kcal/mol) for the addition of water seems to be a consequence of factors other than the exothermicity of the reaction (only 24.5 kcal/mol from complex 16). The activation energy for the fragmentation of the ethyl ester 4b is 25.43 kcal/mol,<sup>28</sup> which suggests that the experimental exothermicity for the addition of water to 3a to yield 5a' might be approximately 25 kcal/mol, in qualitative agreement with the calculated value. For comparison, the Diels–Alder reaction of butadiene and ethene is exothermic by 40.5 kcal/mol<sup>30</sup> and has a substantial activation energy of 27.5 kcal/mol.<sup>31</sup> The dimerization of ketene, which is exothermic by 23 kcal/mol,<sup>32</sup> has a barrier of 31 kcal/mol.<sup>33</sup> The nature of the barriers for the reactions in eq 2 will be discussed in more detail below.

Two views of the MP2/6-31G\* transition structure 17 for the addition of water to 3a are shown in Figure 1A. The most striking feature is the nearly perfect planarity of the entire system. The only atom which is found significantly out of the plane of the molecule is the "spectator" hydrogen (H<sub>10</sub>) on the water. This geometry can be rationalized by considering the HOMO–LUMO interactions between water and 3a. The LUMO of 3a is the in-plane C<sub>2</sub>=O<sub>1</sub> of the ketene. Thus, if the HOMO of the water is an sp<sup>3</sup> lone pair and adds in the plane of 3a, it twists the spectator hydrogen out of plane.

This nearly planar transition structure is a dramatic contrast to other pericyclic reactions, where the transition states are usually nonplanar so as to maximize orbital overlap. For example, in Diels–Alder reactions, the dienophile approaches the diene above the molecular plane of the latter, allowing the two π-systems to overlap.<sup>22a,34</sup> Similar nonplanarity is also calculated for electrocyclicizations,<sup>17</sup> (*vide supra*) sigmatropic rearrangements,<sup>22a</sup> and

cheletropic fragmentations.<sup>22b</sup> It should be noted, however, that in the 1,3-dipolar cycloaddition of fulminic acid to acetylene, the calculated transition structure is planar.<sup>35</sup>

In transition structure 17, the forming O<sub>5</sub>–H<sub>9</sub> and C<sub>2</sub>–O<sub>8</sub> bonds are 1.532 and 1.867 Å, respectively. Both bonds are significantly formed in the transition structure, with the C<sub>2</sub>–O<sub>8</sub> only 0.481 Å longer than that in the enol acid 5a and the O<sub>5</sub>–H<sub>9</sub> bond 0.541 Å longer. Thus, bond formation is concerted and only slightly asynchronous, with the nucleophilic addition of water preceding the proton transfer, despite the fact that the reaction began with the proton hydrogen-bonded to O<sub>5</sub> in 16. The O<sub>8</sub>–H<sub>9</sub> bond is lengthened by only 0.057 Å relative to water, suggesting that the proton transfer does not keep pace with the oxygen addition to the ketene. Other geometric changes in the structure suggest that the transition state for this exothermic reaction is early, in accord with the prediction of the Hammond Postulate.<sup>24</sup> The aldehyde (C<sub>4</sub>–O<sub>5</sub>) bond has lengthened by only 20% of the total change on becoming the enol, and the C<sub>3</sub>–C<sub>4</sub> distance is shorter by only 25% of its overall change on becoming a double bond. The ketene is bent 32.49° from linear. While this represents 60% of the overall change in this bond angle between the ketene and the acid, it is also a reflection of the fact that bending of cumulenes is very facile.<sup>36</sup>

**Addition of Formaldehyde to Formylketene.** In this model system, the loss of formaldehyde from 4H-1,3-dioxin-4-one (6a) to give 3a (eq 3) was expected to be less exothermic than the known fragmentation of 6b because formaldehyde lacks the stabilization of acetone.<sup>26</sup> This should translate into a higher calculated activation energy for the model system than that measured for the reaction of 6b.<sup>23,24</sup> The ground-state geometry of the product dioxinone 6a was optimized in C<sub>1</sub> symmetry with no constraints and is shown in Figure 1B. As before, frequency calculations at both the RHF/3-21G and RHF/6-31G\* levels indicated that these were minimum energy structures. Transition structure 18 was located at both the RHF/3-21G and RHF/6-31G\* levels. However, optimization at the MP2/6-31G\* level was more difficult. The standard procedure,<sup>20,21a</sup> which uses the RHF/6-31G\* second derivative data to guide the MP2/6-31G\* optimization, failed to converge on a transition structure. Due to the size of the system, it was impractical to obtain MP2/6-31G\* second derivatives, and a directed grid search was used instead. Beginning with the best structure from the attempted optimizations, the C<sub>2</sub>–O<sub>8</sub> and O<sub>5</sub>–C<sub>9</sub> bonds were fixed, and the rest of the geometry was optimized. The forces on the fixed bonds and the total energy were used to direct the search. In this manner, structure 18 was obtained (Figure 1B), in which the forces on the breaking bonds were less than 0.000 15 hartree/Å. A conservative estimate would be that the bond lengths are optimized to within 0.005 Å of the transition structure.

Experimentally, the formation of acetone and acetylketene (3b) from 6b has a higher activation energy (31.1 kcal/mol, eq 3)<sup>26</sup> than the fragmentations of esters 4b and 4d (25.4 and 22.2 kcal/mol, respectively, eq 3).<sup>28</sup> Such a trend is reproduced in these calculations as well. The MP4(SDQ)/6-31G\*\*/MP2/6-31G\* + ZPE energy of the transition structure 18 is 35.9 kcal/mol above the ring 6a, while the transition structure 17 is 30.9 kcal/mol above the most stable enol conformation 5a'.

A small activation energy of only 10.6 kcal/mol is calculated for the addition of formaldehyde to 3a. However, this is predicted to be significantly higher than the barrier for the reaction with water. This suggests that the selective reaction of an α-oxo ketene with an alcohol in the presence of an aldehyde or ketone should

(29) Presumably the keto tautomer (4a) is again slightly more stable, but its structure was not investigated.

(30) Tardy, D. C.; Ireton, R.; Gordon, A. S. *J. Am. Chem. Soc.* **1979**, *101*, 1508–1514.

(31) Rowley, D.; Steiner, H. *Disc. Faraday Soc.* **1951**, *10*, 198.

(32) Mansson, M.; Nakasi, Y.; Sunner, S. *Acta Chem. Scand.* **1968**, *22*, 171.

(33) Chickos, J. S.; Sherwood, D. E.; Jug, K. *J. Org. Chem.* **1978**, *43*, 1146.

(34) (a) Birney, D. M.; Houk, K. N. *J. Am. Chem. Soc.* **1990**, *112*, 4127–4133. (b) Bernardi, F.; Bottini, A.; Field, M. J.; Guest, M. F.; Hillier, I. H.; Robb, M. A.; Venturini, A. *J. Am. Chem. Soc.* **1988**, *110*, 3050.

(35) Kormornicki, A.; Goddard, J. D.; Schaeffer, H. F., III. *J. Am. Chem. Soc.* **1980**, *102*, 1763.

(36) (a) Trinquier, G.; Malrieu, J.-P. *J. Am. Chem. Soc.* **1987**, *109*, 5303–5315. (b) Kormornicki, A.; Dykstra, C. E.; Vincent, M. A.; Radom, L. *J. Am. Chem. Soc.* **1981**, *103*, 1652–1656. (c) Brown, R. D.; Champion, R.; Elmes, P. S.; Godfrey, P. D. *J. Am. Chem. Soc.* **1985**, *107*, 4109–4112. (d) Brown, R. D.; Dittman, R. G. *Chem. Phys.* **1984**, *83*, 77–82.

be possible.<sup>37</sup> Since the addition of formaldehyde is slightly more exothermic than the addition of water (25.3 vs 20.9 kcal/mol for the complex **16** yielding the initially formed enol **5a**), if the reactions are considered to be "similar", then the trend in the activation energy runs counter to the Bell–Evans–Polanyi principle<sup>23</sup> and the Hammond Postulate.<sup>24</sup> A better correlation may be found by comparing the relative atomic charges on the oxygens of water and formaldehyde. The Mulliken charge<sup>38</sup> on the oxygen in water is  $-0.87$  and in formaldehyde is  $-0.42$ . The greater negative charge on the water oxygen appears to be associated with greater nucleophilicity and hence a more asynchronous transition structure and a lower barrier.

Two views each of the MP2/6-31G\* structure of dioxinone **6a** and the transition structure **18** are shown in Figure 1B. The overall conformations of the two structures are remarkably similar, as can be seen most clearly in the side views. All of the atoms are nearly in the same plane, with the exception of H<sub>11</sub>. In both, the O<sub>9</sub>–H<sub>11</sub> bond is approximately normal to the plane of the molecule. Although this is a striking example of a least motion pathway, the similarity between **6a** and **18** is to some degree accidental. The nonplanar conformation of the dioxinone ring (**6a**) allows for staggering at the sp<sup>3</sup> hybridized center, C<sub>9</sub>. However, the transition structure **18** has longer bonds and thus fewer steric constraints. The geometry is instead controlled by the orbital interactions. The HOMO of formaldehyde is a lone pair (O<sub>8</sub>), and this is the nucleophilic site which adds in the plane at C<sub>2</sub> of the ketene. In turn, the in-plane lone pair on O<sub>5</sub> of the ketene acts as a nucleophile and adds at C<sub>9</sub> to the π\* of the formaldehyde. On formaldehyde, these two orbitals are orthogonal; therefore, the structure is twisted so as to best accommodate both sets of interactions. In contrast, in the hetero-Diels–Alder reaction of butadiene and formaldehyde<sup>41</sup> and in the ene reaction of formaldehyde and propene,<sup>42</sup> the calculated transition structures involve only the π-system of formaldehyde.

The only significant changes between the transition structure **18** and the dioxinone **6a** are the lengths of the forming bonds. This is an asynchronous transition structure, with the C<sub>2</sub>–O<sub>8</sub> bond more formed than the O<sub>5</sub>–C<sub>9</sub> bond. However, compared to the reactions with water (*vide supra*), this is less asynchronous, with the former 0.626 Å longer in **18** than in **6a** and the latter 0.669 Å longer in **18** than in **6a**. In the reactions with both water and formaldehyde, the asynchronicity indicates that in the addition of a substrate to **3a**, nucleophilic addition to the ketene carbon (C<sub>2</sub>) slightly precedes electrophilic addition to C<sub>9</sub>. The remainder of the bond distances in **18** are consistent with an early transition structure for the exothermic addition of formaldehyde. The four atoms from formaldehyde remain nearly planar in **18**, their root mean square deviation from planarity is only 0.036 Å, while in **6a** the deviation is 0.166 Å. The only other major geometrical change in **18** is the O<sub>1</sub>–C<sub>2</sub>–C<sub>3</sub> angle, which has changed 49%, but as discussed above, this reflects the facile bending of the cumulenes.<sup>36</sup>

**Ring Closure of Formylketene and Acetylketene.** The transition structure **14a** for the ring closure of **3a** to the β-lactone **2a** was previously located at the RHF/6-31G\*\* level by More O'Ferrall et al. (eq 6).<sup>16</sup> In view of the unusual planar transition structure and to provide a comparison with the results obtained for the

above reactions, the geometries of **15a** and **14a** were reoptimized at the MP2/6-31G\* level, and these structures are shown in Figure 1C. This lowered the calculated (MP4(SDQ)/6-31G + ZPE, Tables 1 and 2) activation energy as compared to the RHF/6-31G\* optimization of More O'Ferrall et al.,<sup>16</sup> placing the transition structure **14a** only 2.5 kcal/mol above the ring-closed species **15a**. This is a remarkably low barrier, especially in light of the calculated exothermicity of only 18.9 kcal/mol for the ring opening. Of the three reactions discussed thus far, this has both the lowest calculated exothermicity and the lowest activation energy.

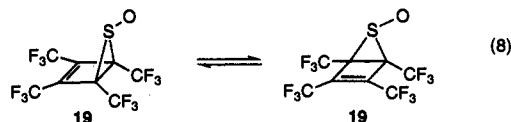
The effects of methyl substitution on the ring-opening reaction were also examined with RHF/6-31G\* geometry optimizations and single-point MP4(SDQ)/6-31G\* + ZPE energies. The structures of acetylketene (**3b**) and the methyl β-lactone (**15b**) and the transition structure between them (**14b**) are shown in Figure 1D. There is again only a very small barrier of 3.2 kcal/mol for the ring opening (Table 1). This is marginally higher than the barrier of 2.5 kcal/mol calculated at this level for the unsubstituted case. Ring opening of **15b** is predicted to be slightly less exothermic (15.9 kcal/mol) than in the unsubstituted case. This may reflect destabilization of acetylketene due to steric repulsion between the methyl group and H<sub>6</sub>. In comparing the ring openings of **15a** and **15b**, the Bell–Evans–Polanyi principle<sup>23</sup> and the Hammond Postulate<sup>24</sup> are followed, and the more exothermic reaction has the lower barrier.

The breaking bond in **14a** is 1.726 Å, which is only 0.236 Å longer than that in the lactone **15a**. Similar distances are found in **14b** and **15b**. The methyl substitution of **14b** provides an independent means of classifying the transition structure as early or late. In the lactone **15b**, a methyl hydrogen is eclipsed with the C<sub>3</sub>–C<sub>4</sub> double bond, while in acetylketene (**3b**), a methyl hydrogen is eclipsed with the C<sub>4</sub>–O<sub>5</sub> double bond. In the transition structure **14b**, the methyl hydrogen is eclipsed with the C<sub>3</sub>–C<sub>4</sub> bond, qualitatively, similar to the lactone **15b**. Early transition structures for these exothermic reactions are thus implied.

While transition structures **18** and **17** are only approximately planar, transition structures **14a** and **14b** have C<sub>s</sub> symmetry and thus appear to be "purer" examples of the tendency of formylketene to participate in planar reactions. When compared to more conventional electrocyclic ring openings, however, the planarity is striking and completely unexpected (*vide supra*). Orbital symmetry predicts<sup>15</sup> and calculations confirm<sup>17a,b,22a</sup> that the allowed ring openings of cyclobutenes proceed via a conrotatory pathway, to allow the breaking σ-bond to overlap with the π-bond.

### Pseudopericyclic Reactions

The planarity of these transition structures is best understood by considering the reactions as "pseudopericyclic", a term which was coined by Lemal et al.<sup>43</sup> to describe pericyclic reactions in which there was a "disconnection in the cyclic array of overlapping orbitals".<sup>44</sup> This originated in the context of the facile degenerate rearrangement of **19** (eq 8), which renders the CF<sub>3</sub> groups equivalent by NMR. The authors proposed that the extraordi-



narily low activation energy (6.8 kcal/mol) for this reaction was

(43) Ross, J. A.; Seiders, R. P.; Lemal, D. M. *J. Am. Chem. Soc.* **1976**, *98*, 4325–4327.

(44) Their full description of a pseudopericyclic reactions was: "a concerted transformation whose primary changes in bonding compass a cyclic array of atoms, at one (or more) of which nonbonding and bonding atomic orbitals interchange roles. In a crucial sense, the role interchange means a 'disconnection' in the cyclic array of overlapping orbitals because the atomic orbitals switching functions are mutually orthogonal. Hence pseudopericyclic reactions cannot be orbital symmetry forbidden."<sup>43</sup>

(37) Note added in proof: this prediction is supported by preliminary competition studies which indicate that **3b** reacts much faster with 1-butanol than with cyclohexanone.

(38) We are aware of the problems associated with the use of Mulliken charges,<sup>21a,39</sup> but the use of other methods to assign atomic charges also presents difficulties.<sup>40</sup>

(39) Breneman, C. M.; Wiberg, K. B. *J. Comput. Chem.* **1990**, *11*, 361–373.

(40) (a) Perrin, C. L. *J. Am. Chem. Soc.* **1991**, *113*, 2865–2868. (b) Birney, D. M. *J. Org. Chem.* **1994**, *59*, 2557–2564.

(41) McCarrick, M. A.; Wu, Y.-D.; Houk, K. N. *J. Am. Chem. Soc.* **1992**, *114*, 1499–1500.

(42) Loncharich, R. J.; Houk, K. N. *J. Am. Chem. Soc.* **1987**, *109*, 6947–6952.

due to the orbital topology on the sulfur, which allows the nonbonding orbital to begin to form a bond while an orthogonal bond is cleaved. However, there is a difficulty with Lemal's example in that his orbital description is not unique. It is possible to mix the bonding and nonbonding orbitals on sulfur and thus produce a new set of orbitals, one of which overlaps with both the breaking and the forming bonds. In part because of this ambiguity, this concept has not been extensively examined, although there have been a few semiempirical calculations on the rearrangement of **19**.<sup>45</sup> The conclusion of these studies was that a transition state with zwitterionic character was implicated instead. A related concept is cruciconjugation, as proposed by Dewar.<sup>46</sup> This has been applied in particular to the bonding in cyclotriphosphazenes, in which the involvement of the phosphorus d-orbitals was suggested to introduce an orthogonality between two bonding molecular orbitals on the phosphorus and thus disconnect the cyclic  $\pi$ -system into noninteracting segments. Here, again, there is an ambiguity in the choice of orbitals. Inclusion of the p-orbitals on phosphorous removes the orthogonality, and, furthermore, the (specific and arbitrary) orientation of the d-orbital is crucial for the theory.

The transition states **14a**, **14b**, **18**, and **17** calculated here provide unambiguous examples of pseudopericyclic reactions. They all clearly satisfy Woodward and Hoffmann's original definition of pericyclic reactions;<sup>15</sup> the breaking and forming bonds are around the perimeter of the ring.<sup>14</sup> However, the unusual planarity or near planarity of the transition structures requires that the orbital interactions are qualitatively different from those commonly encountered in pericyclic reactions. Figure 3 shows a representative system, the approximately symmetric and antisymmetric basis orbitals (with respect to the molecular plane) undergoing bonding changes for the reactants **3a** and water, the transition structure **17**, and product **5a** from Figure 2. The antisymmetric ( $\pi$ ) orbitals are occupied by six electrons, and the symmetric ( $\sigma$  and  $\pi$ ) orbitals are occupied by eight electrons, for a total of 14. The most noticeable feature of these diagrams is that the basis orbitals in antisymmetric system are unchanged from reactants to products. There is a formal shift of an electron from the lone pair on the ketene oxygen ( $O_1$ ) in **3a** to the ether oxygen ( $O_5$ ) in **5a** during the course of the reaction, but the  $\pi$ -orbitals remain the same. Similarly, there is a smooth transformation of the symmetric occupied orbitals from the reactants to the products.

The dramatic, qualitative difference between the transition structure (**17**) and those found for other pericyclic reactions is that the approximate planarity of **17** ensures that there is little or no overlap between the  $\pi$  (antisymmetric) and  $\sigma$  (symmetric) systems in this transition structure. Thus, there is no closed loop of interacting orbitals. Significantly, the Woodward–Hoffmann rules,<sup>15</sup> Fukui's rules based on frontier molecular orbital arguments,<sup>47</sup> and Dewar–Zimmerman transition-state aromaticity arguments<sup>48</sup> all become irrelevant because of this lack of cyclic overlap. For the orbital symmetry rules, the presence of orthogonal orbitals means neither suprafacial nor antarafacial overlap is involved. In frontier molecular orbital theory, the possibility of enforced antibonding HOMO–LUMO overlap is eliminated, and for the aromatic transition-state formalism, aromaticity is irrelevant without a closed loop of orbitals.<sup>49</sup> It

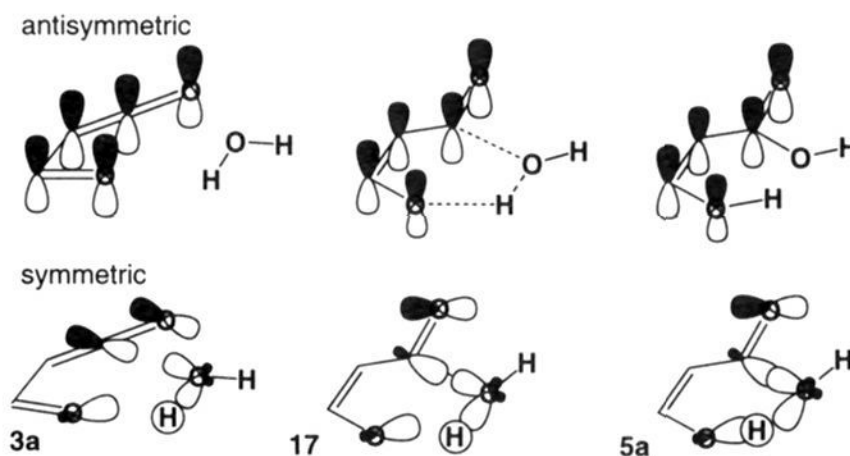


**Figure 3.** Basic atomic orbitals involved in the bonding changes occurring on the addition of water to **3a**. Those which are symmetric and antisymmetric to the  $\sigma$ -plane of the molecules are shown. Note that **17** is only approximately planar.

is important to note that the theories underlying the first two approaches are sufficiently general that they are independent of any specific orbital overlap. It is **only** the constraint imposed when the orbitals overlap in a closed loop that leads to the well known rules and the familiar pattern of alternating forbidden and allowed reactions as the number of electrons is increased.<sup>51</sup>

Therefore, a pseudopericyclic reaction is allowed regardless of the number of participating electrons, just as the stability of an acyclic conjugated polyene does not depend on the number of  $\pi$ -electrons. This prediction is supported by the experimentally observed [4 + 2] cycloaddition of vinyl ethers to  $\alpha$ -oxo ketenes (**3**) to give **7** (eq 2).<sup>1c,2n</sup> In this case, the vinyl ether contributes two electrons, for a total of 12 electrons participating in the bonding changes, while there are 14 electrons involved in transition structure **17** (cf. Figure 3). This is not an exception to the principle of conservation of orbital symmetry. The only approximate symmetry element in the reactant **16**, transition structure **17**, and product **5a** is the  $\sigma$ -plane. Because no electrons shift from symmetric to antisymmetric orbitals, the orbitals correlate, and the reaction is clearly orbital symmetry allowed, regardless of the number of electrons involved.<sup>53</sup>

If pseudopericyclic reactions are allowed but are not stabilized by transition-state aromaticity, how then can the barriers be so low? The answer is that, fundamentally, *neither are they destabilized by aromaticity*. Any closed loop of orbitals which contains  $4n + 2$  electrons (where  $n = 1, 2, 3, \dots; n \neq 0$ ) must have destabilizing as well as stabilizing orbital interactions as a result of the closed loop. Following Goldstein and Hoffmann,<sup>54</sup> consider the occupied orbitals from a system of six p-orbitals. (A figure is provided in the supplementary material.) As an acyclic, conjugated system, they form the  $\pi$  molecular orbitals of 1,3,5-hexatriene. As a cyclic system, they become the  $\pi$  molecular orbitals of benzene. One may argue that the overall aromatic stabilization arises from the fact that first and third  $\pi$  molecular orbitals are stabilized in benzene relative to hexatriene, but the second  $\pi$ -MO is raised in energy. This is due to enforced electron–electron repulsions when the ends of the latter orbital overlap. Houk has similarly argued that the origin of the barrier in pericyclic reactions arises from unavoidable electron–electron repulsions.<sup>55</sup> However, in the [4 + 2] reactions of  $\alpha$ -oxo ketenes, the lack of a cyclic array of overlapping orbitals means that

(45) Snyder, J. P.; Halgren, T. A. *J. Am. Chem. Soc.* **1980**, *102*, 2861–2863.

(46) Dewar, M. J. S.; Healy, E. F.; Ruiz, J. *Pure Appl. Chem.* **1986**, *58*, 67–74.

(47) Fukui, K. *Acc. Chem. Res.* **1971**, *4*, 57.

(48) (a) Dewar, M. J. S. *Angew. Chem., Int. Ed. Engl.* **1971**, *10*, 761. (b) Zimmerman, H. E. *Acc. Chem. Res.* **1971**, *4*, 272.

(49) A referee has pointed out that the configuration mixing (CM) model of Pross and Shaik<sup>50</sup> also is consistent with this interpretation. We note that "the role of symmetry in cycloaddition reactions manifests itself in the CM model in essentially the same way as in the Woodward–Hoffmann approach."<sup>50b</sup>

(50) (a) Pross, A.; Shaik, S. S. *Acc. Chem. Res.* **1983**, *16*, 363–370. (b) Pross, A. In *Advances in Physical Organic Chemistry*; Gold, V., Bethell, D., Eds.; Academic Press: London, 1985, Vol. 21, pp 99–196.

(51) For example, a [2 + 2] cycloaddition is forbidden, while a [4 + 2] cycloaddition is allowed. This is "textbook" knowledge; Lowry and Richardson define pericyclic reactions as: "processes characterized by bonding changes taking place through reorganization of electron pairs within a closed loop of interacting orbitals"<sup>52</sup> (emphasis ours).

(52) Lowry, T. H.; Richardson, K. S. *Mechanism and Theory in Organic Chemistry*, 3rd ed.; Harper and Row, Publishers: New York, 1987; p 839.

(53) The [2 + 2] cycloreversion mechanism in Scheme 1 has a loop of interacting orbitals and is forbidden.

(54) Goldstein, M. J.; Hoffmann, R. *J. Am. Chem. Soc.* **1971**, *93*, 6193–6204.

(55) Houk, K. N.; Gandour, R. W.; Strozier, R. W.; Rondan, N. G.; Paquette, L. A. *J. Am. Chem. Soc.* **1979**, *101*, 6797–6802.



electron–electron repulsions are *not* enforced by the orbital overlap and can be avoided if the electronic interactions are appropriate.

If in these reactions, electron–electron repulsions can be avoided, in what sense are they? They are avoided by the matching of electron densities in the relevant species. Consider the addition of water to **3a**. The central carbon of the ketene ( $C_2$ ) is very electrophilic, and the lone pair on the aldehyde ( $O_3$ ) is nucleophilic. This pattern is complemented by the nucleophilic lone pair and the electrophilic hydrogen from water (or the oxygen and carbon from formaldehyde), each of which is attracted to the matching site on the  $\alpha$ -oxo ketene. These attractions are synergistic, in that as the oxygen from water adds to the ketene, this increases the electron density in the in-plane orbital. Rather than accumulating on the carbonyl oxygen ( $O_1$ ), this negative charge is dispersed by the orthogonal  $\pi$ -system to  $O_3$  at the other end of the molecule. This increases the nucleophilicity of  $O_3$  and enhances its attraction for the hydrogen from water ( $H_9$ ). Thus there is no accumulation of charge and electron–electron repulsion is minimal.<sup>56</sup> These, then, are the stabilizing interactions, not transition-state aromaticity.

### Conclusion

Transition structures for the addition of water and formaldehyde to formylketene (**3a**) (MP2/6-31G\*) have been located. The barrier for the former is predicted to be 4.3 kcal/mol lower than that for the latter, indicating a selectivity which may be of synthetic utility. The calculated activation energies for the reverse reactions reproduce the trends in similar experimental reactions. A transition structure for the hypothetical ring closure of **3a** to give **15a** has also been located at the MP2/6-31G\* level. All the transition structures of these concerted, slightly asynchronous reactions are essentially planar and do not show significant  $\sigma$ – $\pi$  overlap. The orbital topologies are best described as pseudopericyclic reactions, a novel class of pericyclic reactions in which (to paraphrase Lemal et al.<sup>43</sup>) there is no closed loop of interacting orbitals because there is a “disconnection” in the orbital overlap around the complete ring of breaking and forming bonds due to mutually orthogonal orbitals. This means that the number of  $\pi$ -electrons participating does not influence the “allowedness” of

(56) The same argument may be made for the ring closure of **3** to **15**.

the reaction. Paradoxically, although pseudopericyclic reactions cannot be orbital symmetry forbidden, neither can they experience the transition-state aromaticity commonly invoked to stabilize orbital symmetry-allowed pericyclic reactions. Yet pseudopericyclic reactions can have very low activation energies due to the lack of enforced electron–electron repulsions which are found in so-called aromatic transition states. This is clearly evidenced by the very low barriers calculated for many of the reactions of **3a**. Although the geometries of the transition structures are early for these exothermic reactions, in accord with the Hammond Postulate, the exothermicity does not correlate with barrier heights across the range of reactions examined. Rather, the magnitude of the barriers can be understood in terms of favorable nucleophilic/electrophilic or atomic charge interactions. Thus, the contrast between pericyclic and pseudopericyclic reactions provides new insights into the fundamental nature of allowed and forbidden reactions and into the origin of barriers to reactions. Based on these considerations, efforts are underway in this laboratory to design other  $4n$  and  $4n + 2$  systems with low barriers as well as to test the predicted relative rates of addition of  $\alpha$ -oxo ketenes with alcohols and aldehydes or ketones.

**Acknowledgment.** It has been a pleasure to collaborate with J. Stewart Witzeman, whose experimental studies provided the impetus for this work. The calculations were carried out using grants of computer time from Texas Tech University, the Pittsburgh Supercomputing Center, and Eastman Kodak Company at the National Center for Supercomputing Applications. Their support is gratefully acknowledged. Acknowledgment is made to the donors of The Petroleum Research Fund, administered by the American Chemical Society, for partial support of this research. The Advanced Research Program of the State of Texas provided additional support for this project.

**Supplementary Material Available:** Optimized Cartesian coordinates for all structures are provided, as is a figure correlating the  $\pi$ -orbitals of hexatriene with those of benzene (3 pages). This material is contained in many libraries on microfiche, immediately follows this article in the microfilm version of the journal, and can be ordered from the ACS; see any current masthead page for ordering information.